Tissue Regeneration and Wound Repair Using Conductive Bioelectric Wound Dressings Containing Cationic Fentonite

Darlene McCord, Ph.D., Michael Lavor, MD, Steven Kravitz, DPM, Robert Frykberg, DPM

Abstract

Conductive bioelectric wound dressings containing a blend of cations, known to be required during the transition between the inflammatory stage and remodeling, are effective in treating complex wounds. The dressings are based on fentonite technology. Fentonite is a rare natural blend of cations with a high cationic exchange capacity and a high oxygen-reactive potential. In independent testing, fentonite-based dressings eliminated biofilms within 24 hours and killed wound pathogens in three hours or fewer. A 198-patient study of acute and chronic wounds proved that fentonite-based conductive bioelectric wound dressings reduced healing times and resolved stalled chronic wounds, usually in less than 90 days. The dressing is noncytotoxic because fentonite dressings work by balancing ions in the wound environment. This is a significant advantage of wound dressings that contain antibiotics or antiseptics.

Introduction

Conductive bioelectric nanomaterials, such as fentonite and other cationic nanomaterials, have emerged as promising new agents in wound healing and skin tissue engineering. These nanomaterials integrate with advanced polymer delivery systems, offering a multifaceted approach to fostering improved solutions. Developing and utilizing conductive bioelectric nanomaterials represents a significant stride in modern medical science.[1-4]

The past failure to consider incorporating bioelectric medicine into standard-of-care medicine has resulted from reliance upon external medical devices providing an electrical charge through wires or remote devices. Such medical devices are not well received by patients and have not been reliable because of the current variances that deliver nonpredictable results because of their proximity to the target organ.[5-6]

The field of bioelectric medicine has seen the introduction of nanomaterials that come into direct contact with the target organ without relying on external stimulation. Bioelectric nanomaterial-based wound dressings, engineered to possess similar conductivity to human skin, represent a groundbreaking advancement in wound care. By mimicking the natural electrical properties of living tissues, these innovative dressings offer a unique approach to enhancing wound healing, significantly improving patient outcomes.[7-9]

The conductivity of these bioelectric-based dressings is a critical factor in their efficacy. The human skin exhibits intrinsic electrical conductivity, crucial in various physiological processes, including wound healing. By replicating this conductivity, conductive bioelectric dressings create a microenvironment that closely resembles the natural electrical milieu of the skin, facilitating more efficient tissue regeneration.[10]

Resistance to traditional antibiotics and antiseptics is due to persister cells' protective and survival abilities. Persister cells are pathogens that have become metabolically inactive and, in doing so, have developed a more resistant outer wall membrane that serves as a shield. Even after a wound has been debrided, persister cells are not removed. Once a persister cells sense, through the release of autoinducers, that the level of pathogens has fallen below a quorum, they quickly convert to replicating pathogens and resupply the wound with adequate pathogens to recolonize the wound. The ability of bioelectric nanomaterial-based dressings to block this resurgence of bacterial activity is their ability to block the release of autoinducers released by pathogens, including persister cells.[11-12]

CHRONIC PATHOGEN COUNT POTENTIAL PER 2 SQUARE INCHES OF WOUND

	Bacteria Count	Time (hours)
Stage 1	50	0.017
	100	2.317
	200	4.617
	400	6.917
	800	9.217
	1,600	11.517
	3,200	13.817
	6,400	16.117
	12,800	18.417
	25,600	20.717
	51,200	23.017
	102,400	25.317
	204,800	27.617
	409,600	29.917
Stage 2	819,200	32.217
	1,638,400	34.517
Stage 3	3,276,800	36.817
Stage 4	6,553,600	39.117
	13,107,200	41.417
	26,214,400	43.717
Stage 5	52,428,800	46.017

	Bacteria Count	Time (hours)
Stage 1	100	0.017
	200	2.317
	400	4.617
	800	6.917
	1,600	9.217
	3,200	11.517
	6,400	13.817
	12,800	16.117
	25,600	18.417
	51,200	20.717
	102,400	23.017
	204,800	25.317
	409,600	27.617
Stage 2	819,200	29.917
	1,638,400	32.217
Stage 3	3,276,800	34.517
Stage 4	6,553,600	36.817
	13,107,200	39.117
	26,214,400	41.417
Stage 5	52,428,800	43.717

	Bacteria Count	Time (hours)
Stage 1	1,000	0.017
	2,000	2.317
	4,000	4.617
	8,000	6.917
	16,000	9.217
	32,000	11.517
	64,000	13.817
	128,000	16.117
	256,000	18.417
Stage 2	512,000	20.717
	1,024,000	23.017
	2,048,000	25.317
Stage 3	4,096,000	27.617
Stage 4	8,192,000	29.917
	16,384,000	32.217
	32,768,000	34.517
Stage 5	65,536,000	36.817

Release of Autoinducers
Colonization
Release of Virulent Factors

Figure 1

There are multiple reasons a wound will recolonize. Persister cells play a significant role in this event. Debridement pushes these cells below the wound bed, where they can repopulate and cause an ongoing infection. A few remaining persister cells can blossom into a contaminated wound within hours.[13] (Figure 1)

At the core of bioelectric wound dressings' efficacy lies their ability to facilitate electrical conductivity, mimicking the natural electrical properties of living tissues. This feature is advantageous as it modulates cellular activities crucial for wound healing, such as cell proliferation, migration, and differentiation. By harnessing electrical signaling pathways, conductive bioelectrical nanomaterials orchestrate the intricate dance of cellular responses necessary for tissue repair.[14]

Ionic Balance

The balance between anions (negatively charged ions) and cations (positively charged ions) is crucial for maintaining the proper functioning of cells, tissues, and wound healing. This ionic balance is essential for all three phases of tissue reconstruction involved with wound closure.

The human body generally strives to maintain electroneutrality, which means the overall charge is balanced. The primary cations in the body include sodium (Na+), potassium (K+), calcium (Ca2+), and magnesium (Mg2+). The significant anions include chloride (Cl−), bicarbonate (HCO3−), and phosphate (HPO4^2−).[15] (Figure 2)

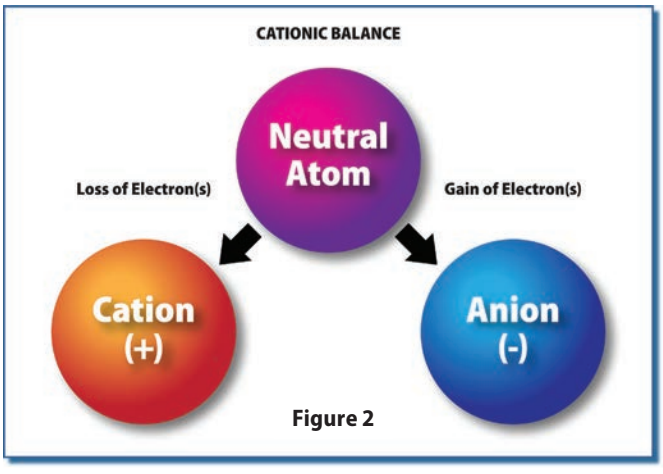

Figure 2

The concentration of ions is usually tightly regulated within cells and the extracellular fluid. In chronic non-healing wounds, the ionic balance is dominated by anions. Pathogens and the biofilms they produce are both anionic. To eliminate them without cytotoxicity, the addition of natural cations is required.[16-17]

It's important to note that the specific concentrations of ions can vary in different tissue compartments (intracellular vs. extracellular). The balance must be intricately regulated to ensure cells' proper functioning and closure of wounds. This is the primary objective of advanced wound healing products. (Figure 3)

The future of wound care and tissue regeneration will focus on ion neutrality or specific ionic balances that favor tissue modeling.

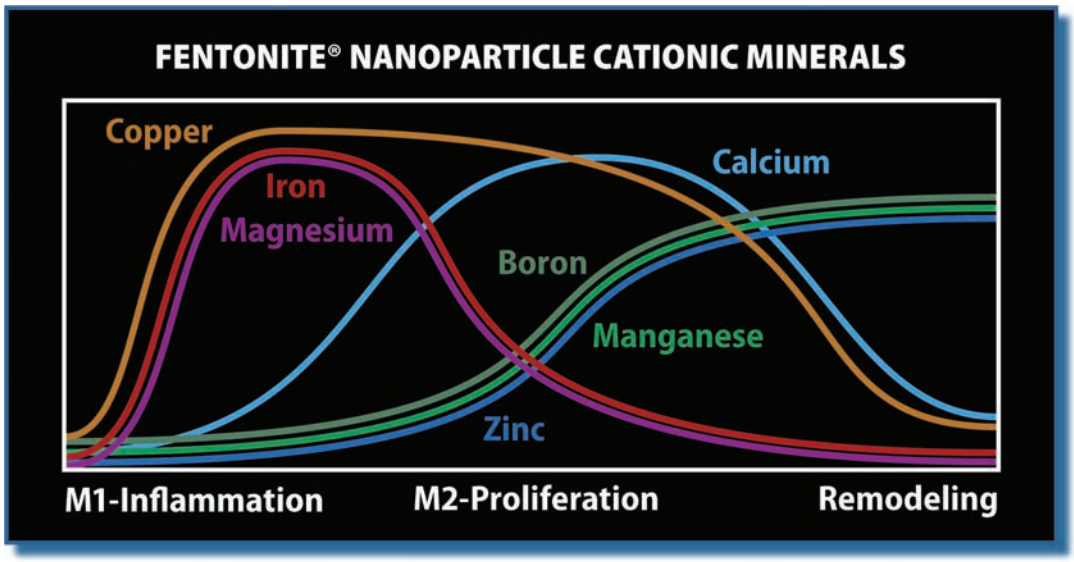

Figure 3

Thermoreversible Micelles for Bioelectric Delivery

In the context of wound management, micelles emerge as remarkable agents capable of orchestrating a multifaceted assault on bacterial reproduction, thereby fostering expedited wound healing. When introduced into wounds, micelles deploy their inherent properties to thwart bacterial proliferation and promote a conducive environment for tissue repair.[18]

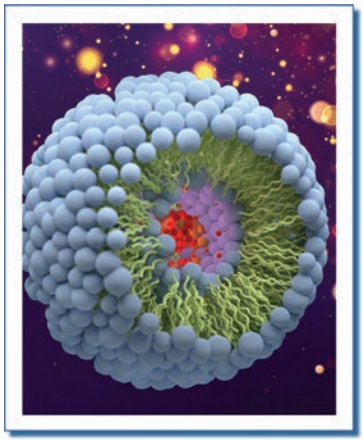

Figure 4

Micelles (Figure 4), characterized by their amphiphilic nature, swiftly interact with the diverse array of lipids and proteins present within wound exudates. Upon encountering bacterial membranes within the wound milieu, micelles embark on a dual-pronged approach to disrupt bacterial reproduction and biofilm structures. Their hydrophobic tails avidly embed within the lipid bilayers of bacterial and biofilm membranes, inducing destabilization and compromising membrane integrity. This disruption culminates in the leakage of vital cellular components, including ions and proteins, thereby impeding essential metabolic processes pivotal for bacterial replication. Importantly, this process frees the iron the bacteria has sequestered as a survival mechanism. The freed iron is then released, causing fatal consequences for the bacteria.[19]

Moreover, micelles exhibit a remarkable capability to sequester essential nutrients and growth factors within the wound environment. By encapsulating proteins and growth factors necessary for bacterial growth and virulence, micelles effectively deprive bacteria of the requisite resources for proliferation. This nutrient deprivation strategy acts as a potent deterrent against bacterial reproduction, fostering an environment conducive to wound healing.[20]

Furthermore, micelles possess inherent antimicrobial properties, attributed to their ability to disrupt membrane potential and interfere with vital cellular processes. By perturbing electrochemical gradients and inhibiting ATP synthesis, micelles impede energy metabolism within bacterial cells, thereby stalling their replicative machinery and curbing proliferation.

The collective actions of micelles in wound environments synergistically impede bacterial reproduction while concurrently fostering an optimal milieu for tissue repair. Micelles emerge as pivotal players in promoting wound healing and

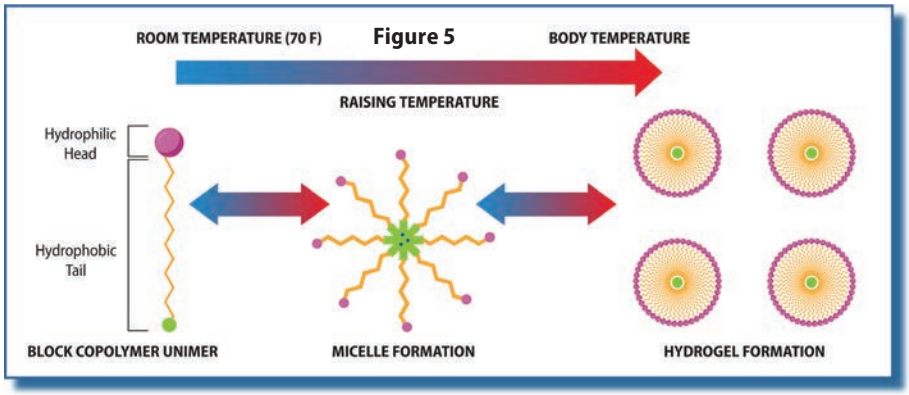

Figure 5

mitigating the risk of wound-associated infections by thwarting bacterial proliferation, sequestering essential nutrients, and exerting antimicrobial effects. Leveraging the therapeutic potential of micelles in wound management underscores their significance as a promising avenue for advancing wound care practices and facilitating patient outcomes.[21]

The fentonite bioelectric activity is delivered through micelle BioBlock technology that also encapsulates a unique preservative system and distributes its decisive action throughout the millions of micelles to ensure long-term protection for the hydrogel against microbial contamination. BioBlock technology is thermoreversible. It is water-thin at 65c and then becomes a thick hydrogel at 98c. The preservative system is a broad-spectrum antimicrobial effective against many bacteria, fungi, and viruses. The preservative distribution throughout the millions of micelles creates a large surface area over which the preservative can act, providing long-term protection against microbial contamination. (Figure 5)

One critical application of conductive bioelectric dressings infused with blends of conductive elements such as fentonite is the ability of specific ionic blends to alter the electrical properties of the wound's environment and influence the wound healing process. Bioelectric dressings promote enhanced cell adhesion and extracellular matrix deposition, fostering improved tissue regeneration by creating a conductive microenvironment at the wound site.

Bioelectric nanomaterial-based dressings actively combat microbial infections, a prevalent challenge in wound management. The inherent antimicrobial properties of specific conductive ionic blends, coupled with their ability to bind anionic pathogens, contribute to eradicating pathogens while promoting tissue repair—a dual-action approach crucial for successful wound healing of chronic wounds.[22] (Figure 6)

Fentonite Conductive Bioelectric Wound Dressings

Fentonite's conductive bioelectric activity additionally provides a non-cytotoxic approach to inhibiting wound infections and biofilm formation by blocking the activity of ionically charged autoinducers. Bacteria first release autoinducers while they are still in their pre-infection state. Autoinducers are signaling molecules produced and released by bacteria as they grow and reach a specific cell density within the biofilm. When the concentration of autoinducers reaches a threshold

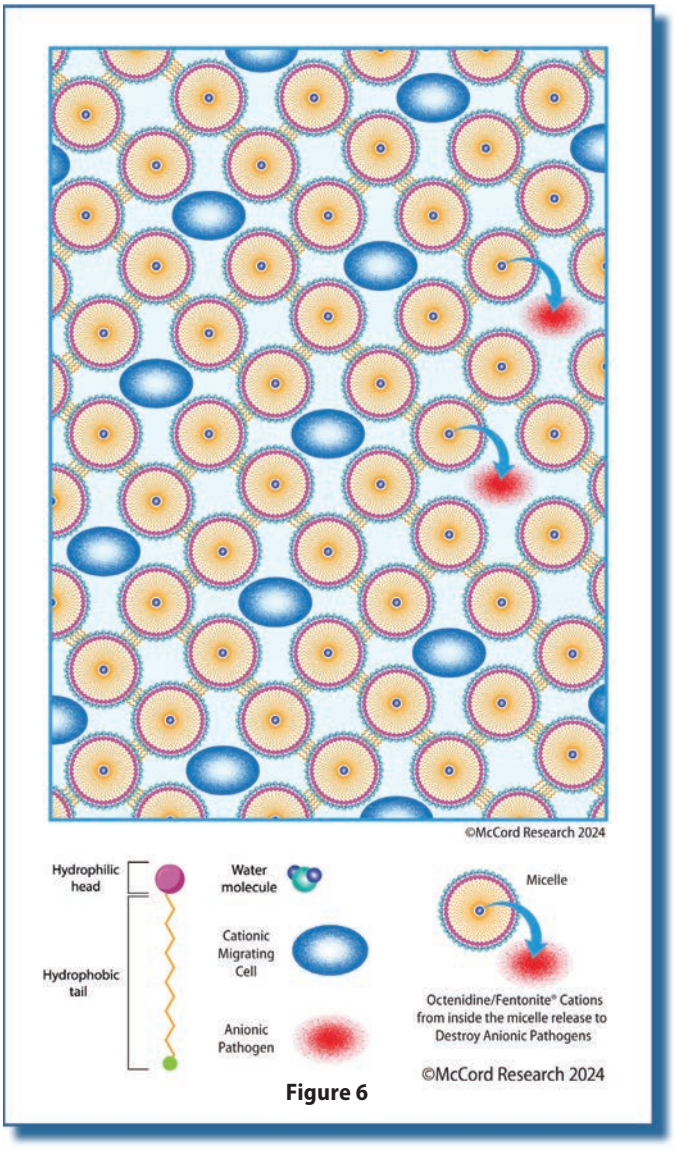

Figure 6

level, they bind to special receptors on bacterial cells, initiating a signaling cascade that activates quorum sensing.

Materials and Methods

Fentonite (test article) was stored at room temperature upon arrival. The test article was weighed (400 mg) and resuspended in 1 ml of sterile water. 500 µL of each prepared test article was added to 500 µL of the assay medium for the NHEK cytotoxicity evaluations. For the HFF cytotoxicity evaluations, 250 µL of each prepared test article was added to 750 µL of assay medium. Two hundred microliters (200 µL) of the 200 mg/ml solution (NHEK) or 100 mg/ml solution (HFF) were transferred to 800 µL of assay medium (1:5 dilution) for a total of nine serial dilutions. One hundred microliters of each 2x concentration were added in triplicate wells to the cells containing 100 µL of fresh assay medium for cytotoxicity evaluation. Staurosporine was purchased from Sigma Aldrich (St. et al.) and evaluated as a positive control compound in the cytotoxicity assays.

Cytotoxicity Evaluations

HFF Cell Culture: Normal human foreskin fibroblasts (ATCC SCRC-1041) were cultured in DMEM supplemented with 10% heat-inactivated fetal bovine serum, two mM L glutamine, 100 U/ml penicillin and 100 µg/ml streptomycin. Cells were seeded in flat bottom 96 healthy microtiter plates at 5 x 103 cells per well and incubated at 37°C/5% CO2 overnight for adherence. Following overnight incubation, the cell culture medium was removed and replaced with 100 µL per well of medium. The compound was added in triplicate wells to the cells at 100 µL per well. Compound plus medium allow was evaluated as a colorimetric control in a single well.

NHEK Cell Culture: Normal human epidermal keratinocytes (Lonza 00192906) were cultured in KGM Gold Keratinocyte medium with supplied growth supplements. Cells were seeded in flat bottom 96 healthy microtiter plates at 2 x 104 cells per well and incubated at 37°C/5% CO2 overnight for adherence. Following overnight incubation, the cell culture medium was removed and replaced with 100 µL per well of medium. The compound was added in triplicate wells to the cells at 100 µL per well. Compound plus medium allow was evaluated as a colorimetric control in a single well per concentration.[24] (Figures 7 & 8)

Figure 7

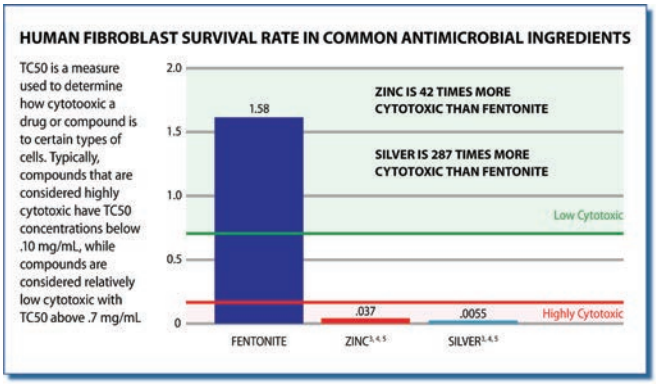

Figure 8

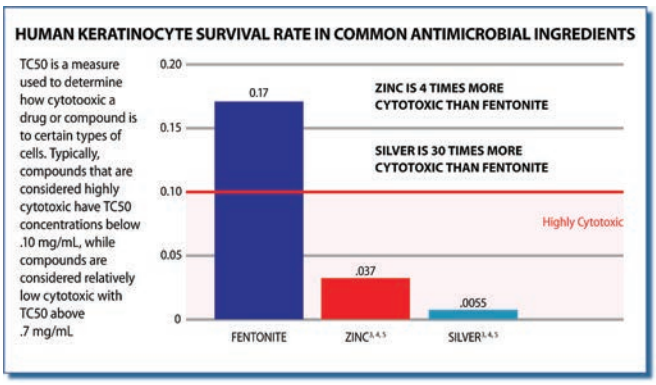

Autoinducers play a crucial role in the initiation and regulation of biofilm formation. As bacteria produce autoinducers, the increasing concentrations signal a sufficiently dense bacterial population. This triggers the production of extracellular polymeric substances (EPS), responsible for the biofilm's structural integrity. Autoinducers help synchronize the timing of biofilm formation, ensuring the biofilms mature collectively.

Autoinducers are at the front end of the cascade. Through a process known as quorum sensing, autoinducers continue to collect until the bacteria "sense" there are enough bacteria to release virulent factors. The biofilm forms through the release of EPS, and the infection and biofilm continue to expand until the host is overcome.

Fentonite blocks the infection cascade by overwhelming the bacteria's signaling processes. Bioelectric or cationic dressings overwhelm the bacteria and biofilm or block their origination by infusing excessive cations and disrupting bacteria cell signaling and gene expression.

The cationic minerals in fentonite are native to the wound environment and are part of the normal healing process. As a wound goes through the healing process, it uses cationic minerals. Without these natural minerals, the wound stalls and may transition from healing by primary intention to a stalled chronic wound. Fentonite allows wounds to heal quickly without the cytotoxic use of antibiotics or antiseptics in traditional wound care products.

Materials and Methods

The organisms are prepared by inoculating the surface of Soybean-Casein Digest Agar (TSA) incubated at 32.5 ± 2.5°C for three days. Following the incubation period, the plates are washed with sterile Serological Saline Solution to harvest the microorganisms used, and dilutions with Saline are made, plated on TSA in duplicate, and incubated at 36 ± 1 °C for 42 hours to determine the concentration. The inoculum level is then adjusted to 108 cfu/ mL for use as a stock suspension. Stock suspensions are well mixed and homogenized at inoculation for each organism.

The following microorganisms were used in this Kill Time Study to demonstrate the antimicrobial properties of the Fentonite mixture & Hydrogel Component against common pathogenic organisms: Microbiology Kwik-Stiks Staphylococcus epidennidis ATCC 35984, Escherichia coli ATCC 25922, Candida albicans ATCC 90028, Methicillin Resistant Staphylococcus aureus ATCC 33591, Streptococcus pyogenes ATCC 19615, Pseudomonas aeruginosa 9027, Klebsiella pneumoniae ATCC 10031, and Clostridioides difficile ATCC 700057.

Using Saline, positive controls are performed by pour plating to enumerate inoculum levels and verify culture purity during testing. Negative controls are performed to establish the sterility of media, reagents, and materials used at the initiation. Neutralizer Suitability using Dey-Engley Neutralizing Broth (DEB) is performed concurrently with Kill Time testing to confirm the recovery of< I 00 CFU of the test organism in the subculture media in the presence of the product.

Findings

Accession# 28532 Rev l indicates a 99.9% log reduction at 12, 24, and 48 hours for Staphylococcus epidemics ATCC 35984, Escherichia coli ATCC 25922, Candida albicans ATCC 90028, Methicillin-Resistant Staphylococcus aureus ATCC 33591, Streptococcus pyogenes ATCC 19615, Pseudomonas aeruginosa 9027, Klebsiella pneumoniae ATCC 1003, and Clostridioides difficile ATCC 700057.[25] (Figure 9)

FENTONITE® & BIORELESE® PATHOGEN KILL RATES TEST RESULTS

(MRSA) Staphylococcus aureus ATCC 33591

Exposure Time	Concentration of Organism cfu/mL		Percent Reduction	
	Control	Product	Control	Product
Time 0	2.8 x 10^6	N/A	N/A	N/A
Time 1 Hour	N/A	<100	N/A	99.99%
Time 6 Hours	N/A	<100	N/A	99.99%
Time 12 Hours	N/A	<100	N/A	99.99%
Time 24 Hours	N/A	<100	N/A	99.99%

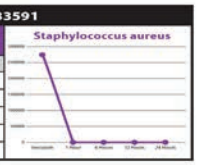

Klebsiella pneumoniae ATTC 13883

Exposure Time	Concentration of Organism cfu/mL		Percent Reduction	
	Control	Product	Control	Product
Time 0	7.0 x 10^6	N/A	N/A	N/A
Time 1 Hour	N/A	4.0 x 10^2	N/A	99.99%
Time 6 Hours	N/A	<100	N/A	99.99%
Time 12 Hours	N/A	<100	N/A	99.99%
Time 24 Hours	N/A	<100	N/A	99.99%

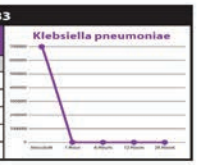

Escherichia coli ATCC 8739

Exposure Time	Concentration of Organism cfu/mL		Percent Reduction	
	Control	Product	Control	Product
Time 0	2.0 x 10^6	N/A	N/A	N/A
Time 1 Hour	N/A	<100	N/A	99.99%
Time 6 Hours	N/A	<100	N/A	99.99%
Time 12 Hours	N/A	<100	N/A	99.99%
Time 24 Hours	N/A	<100	N/A	99.99%

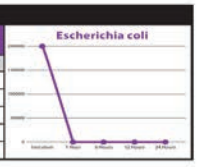

Staphylococcus epidermidus ATCC 12228

Exposure Time	Concentration of Organism cfu/mL		Percent Reduction	
	Control	Product	Control	Product
Time 0	2.4 x 10^6	N/A	N/A	N/A
Time 1 Hour	N/A	<100	N/A	99.99%
Time 6 Hours	N/A	<100	N/A	99.99%
Time 12 Hours	N/A	<100	N/A	99.99%
Time 24 Hours	N/A	<100	N/A	99.99%

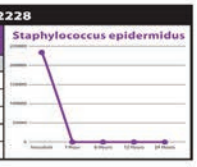

Pseudomonas aeruginosa ATCC 9027

Exposure Time	Concentration of Organism cfu/mL		Percent Reduction	
	Control	Product	Control	Product
Time 0	8.7 x 10^6	N/A	N/A	N/A
Time 1 Hour	N/A	3.0 x 10^4	N/A	99.66%
Time 6 Hours	N/A	1.0 x 10^2	N/A	99.99%
Time 12 Hours	N/A	<100	N/A	99.99%
Time 24 Hours	N/A	<100	N/A	99.99%

Streptococcus pyogenes ATCC 12344

Exposure Time	Concentration of Organism cfu/mL		Percent Reduction	
	Control	Product	Control	Product
Time 0	1.0 x 10^6	N/A	N/A	N/A
Time 1 Hour	N/A	<100	N/A	99.99%
Time 6 Hours	N/A	<100	N/A	99.99%
Time 12 Hours	N/A	<100	N/A	99.99%
Time 24 Hours	N/A	<100	N/A	99.99%

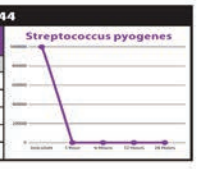

Candida albicans ATCC 10231

Exposure Time	Concentration of Organism cfu/mL		Percent Reduction	
	Control	Product	Control	Product
Time 0	2.0 x 10^6	N/A	N/A	N/A
Time 1 Hour	N/A	3.2 x 10^5	N/A	84.00%
Time 6 Hours	N/A	3.0 x 10^4	N/A	98.50%
Time 12 Hours	N/A	4.0 x 10^3	N/A	99.80%
Time 24 Hours	N/A	<100	N/A	99.99%

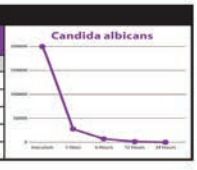

Fentonite® is a rare earth nano-mineral compound that is found in a single remote location. It provides a precise balance of cationic minerals that are embedded in a low pH illite/smectite matrix that effectively traps and deactivates anions, toxins and pathogens. Fentonite effectively chelates and binds toxins in wound exudate and lowers wound pH to create an environment hostile to pathogenic activity.

Figure 9

Antimicrobial Effectiveness Test

USP <51> Antimicrobial Effectiveness Testing involves inoculating five individual test organisms (Staphylococcus aureus ATCC 6538, Pseudomonas aeruginosa ATCC 9027, Escherichia coli ATCC 8739, Candida albicans ATCC 10231 and Aspergillus brasiliensis ATCC 16404) into separate 20 gram aliquots of the test sample. The starting level for each organism is between 100,000 to 1,000,000 organisms. The samples are then incubated at 20-25oC for 28 days. Aliquots are removed from these samples at 7, 14, and 28 days (depending on the product category) to determine recoveries of any remaining viable test organisms to determine preservative effectiveness.

There are 4 Categories listed in USP <51>, and the acceptance criteria for tested organisms for each category.

USP Compendia Product Categories

Category	Product Description
1	Injections; other parenterals including emulsions, otic products, sterile nasal products, and ophthalmic products made with aqueous bases or vehicles
2	Topically used products made with aqueous bases or vehicles; nonsterile nasal products and emulsions, including those applied to mucous membranes
3	Oral products other than antacids, made with aqueous bases or vehicles
4	Antacids made with an aqueous base

USP Acceptance Criteria for Tested Microorganisms

Category	Bacteria	Yeast & Molds
1	Not less than 1.0 log reduction from the initial calculated count at 7 days, not less than 3.0 log reduction from the initial count at 14 days, and no increase from the 14 days' count at 28 days.	No increase from the initial calculated count at 7, 14 and 28 days
2	Not less than 2.0 log reduction from the initial count at 14 days, and no increase from the 14 days' count at 28 days	No increase from the initial calculated count at 14 and 28 days
3	Not less than 1.0 log reduction from the initial count at 14 days, and no increase from the 14 days' count at 28 days	No increase from the initial calculated count at 14 and 28 days
4	No increase from the initial calculated count at 14 and 28 days	

"No increase" in counts is defined as NMT 0.5 log10 unit more than the value to which it is compared.

Other microorganisms may be added to those included within the standard panel. This may consist of microorganisms an environmental monitoring program has isolated from a location within the manufacturing facility or a product containing the organism of concern. Microorganisms isolated in this manner are often more resistant to the microbiocidal effects of the preservative ingredient. One example of a problematic organism for aqueous-based formulations is Burkholderia cepacia, which many are including in their testing.[26] (Figure 10)

Biofilms Inhibit Healing

Biofilms play a significant role in the persistence and exacerbation of chronic wounds, rendering their removal crucial for effective wound management. These complex communities of bacteria, encased within a self-produced extracellular matrix, create a protective environment that shields bacteria from antibiotics, immune responses, and other antimicrobial agents. As a result, biofilms significantly impede wound healing processes and increase the risk of complications.

Firstly, removing biofilms from chronic wounds is essential for mitigating infection. Biofilms act as reservoirs of bacteria, allowing them to persist and increase despite antimicrobial treatments. The presence of biofilms prolongs the inflammatory phase of wound healing and impedes subsequent phases, such as proliferation and remodeling, leading to delayed healing and chronicity.

Biofilms contribute to chronic wound inflammation. They trigger a sustained inflammatory response by releasing pro-inflammatory cytokines and reactive oxygen species, exacerbating tissue damage and impeding cellular activities essential for wound repair. By removing biofilms, clinicians can mitigate this inflammatory burden, facilitating a more conducive environment for healing.

Moreover, biofilms compromise the efficacy of antimicrobial treatments. The protective matrix surrounding biofilm-embedded bacteria limits the penetration of antibiotics and other antimicrobial agents, rendering them less effective or completely ineffective. Consequently, eliminating biofilms is imperative to enhance antimicrobial therapies' efficacy and prevent antibiotic resistance development.

Biofilms impair the functionality of immune cells within the wound bed. The presence of biofilms

FENTONITE® & BIORELESE® PRESERVATIVE EFFECTIVENESS TEST RESULTS

Staphylococcus aureus ATCC 6538

Exposure Time	Concentration of Organism cfu/mL		Percent Reduction	
Product	BioRelese	Fentonite	BioRelese	Fentonite
Inoculum	741,000	741,000	N/A	N/A
Day 2	<10	<100	99.999%	99.99%
Day 7	<10	<100	99.999%	99.99%
Day 14	<10	<100	99.999%	99.99%
Day 21	<10	<100	99.999%	99.99%
Day 28	<10	<100	99.999%	99.99%

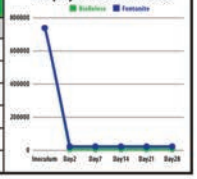

Candida albicans ATCC 10231

Exposure Time	Concentration of Organism cfu/mL		Percent Reduction	
Product	BioRelese	Fentonite	BioRelese	Fentonite
Inoculum	581,000	581,000	N/A	N/A
Day 2	850	<100	99.854%	99.99%
Day 7	<10	<100	99.999%	99.99%
Day 14	<10	<100	99.999%	99.99%
Day 21	<10	<100	99.999%	99.99%
Day 28	<10	<100	99.999%	99.99%

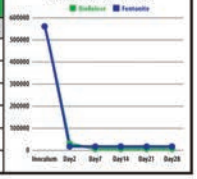

Escherichia coli ATCC 8739

Exposure Time	Concentration of Organism cfu/mL		Percent Reduction	
Product	BioRelese	Fentonite	BioRelese	Fentonite
Inoculum	864,000	864,000	N/A	N/A
Day 2	<10	<100	99.999%	99.99%
Day 7	<10	<100	99.999%	99.99%
Day 14	<10	<100	99.999%	99.99%
Day 21	<10	<100	99.999%	99.99%
Day 28	<10	<100	99.999%	99.99%

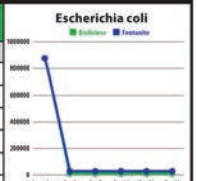

Aspergillus brasiliensis ATCC 16404

Exposure Time	Concentration of Organism cfu/mL		Percent Reduction	
Product	BioRelese	Fentonite	BioRelese	Fentonite
Inoculum	501,000	501,000	N/A	N/A
Day 2	380	<100	99.924%	99.99%
Day 7	<10	<100	99.999%	99.99%
Day 14	<10	<100	99.999%	99.99%
Day 21	<10	<100	99.999%	99.99%
Day 28	<10	<100	99.999%	99.99%

Pseudomonas aeruginosa ATCC 9027

Exposure Time	Concentration of Organism cfu/mL		Percent Reduction	
Product	BioRelese	Fentonite	BioRelese	Fentonite
Inoculum	871,000	871,000	N/A	N/A
Day 2	<10	<100	99.999%	99.99%
Day 7	<10	<100	99.999%	99.99%
Day 14	<10	<100	99.999%	99.99%
Day 21	<10	<100	99.999%	99.99%
Day 28	<10	<100	99.999%	99.99%

Fentonite® is a rare earth nano-mineral compound that is found in a single remote location. It provides a precise balance of cationic minerals that are embedded in a low pH illite/smectite matrix that effectively traps and deactivates anions, toxins and pathogens. Fentonite effectively chelates and binds toxins in wound exudate and lowers wound pH to create an environment hostile to pathogenic activity.

Figure 10

hampers the recruitment and activity of immune cells, compromising their ability to eradicate bacteria and promote wound healing. Therefore, removing biofilms is essential to restore the wound microenvironment's immunological balance and enhance the host's defense mechanisms against infection.

Advanced Bioelectric Micelle Technology with Fentonite and BioBlock Technologies Reduces Biofilms by 99.99%, Wound Pathogens Within 3 Hours or Less, and is Effective Against Repeat Pathogen Inoculation for 28 days.[27]

Biofilm Study

Purpose

The purpose of this study is to evaluate three test articles' ability to prevent the formation of Pseudomonas aeruginosa biofilm using the Colony/Drip Flow Biofilm Reactor (C/DFBR) methodology. Testing will be performed based upon published modifications [Lipp et al, 2010; DOI 10.12968/jowc.2010.19.6.48468 and Stoffel et al, 2020; DOI: 10.1111.wrr.12806] of ASTM E2647-20, Standard Test Method for Quantification of a Pseudomonas aeruginosa Biofilm Grown Using Drip Flow Biofilm Reactor with Low Shear and Continuous Flow.

Testing will be performed by Good Laboratory Practices, as specified in 21 CFR Part 58. Characterizing the identity, strength, purity, composition, stability, and solubility of the test articles remains the responsibility of the Sponsor and will not be performed by the Testing Facility (21 CFR Part 58.105).

Scope

Absorbent pads will be mounted onto glass slides, the prepared slides will be placed into a DFBR, and the DFBR will be sterilized. Sterilized polycarbonate membranes will be placed on top of the absorbent pads, and then the membranes' top surface will be inoculated with Pseudomonas aeruginosa. After a 30-minute air dry, a sterile rubber ring will be placed over the membrane, and 1 mL of the test articles will be dispensed inside the ring before starting a continuous 5 mL/hour flow of dilute growth media into the DFBR at room temperature. An additional

FENTONITE® ELIMINATES BIOFILMS

Replicate	Log_{10} CFU/ Membrane Recovery	Average Log_{10} CFU/ Membrane Recovery	Log_{10} CFU/Membrane Reduction Relative to Untreated Control	Average Log_{10} CFU/ Membrane Reduction Relative to Untreated Control
1	1.60	1.60	7.05	7.05
2	1.60		7.05	
3	1.60		7.05	

Figure 11

1 mL of two test articles will be dispensed inside the ring again after 24 and 48 hours of continuous flow. After 72 hours of constant flow conditions, membranes will be removed, rinsed, and transferred to containers of neutralizing eluent. Biofilm will be

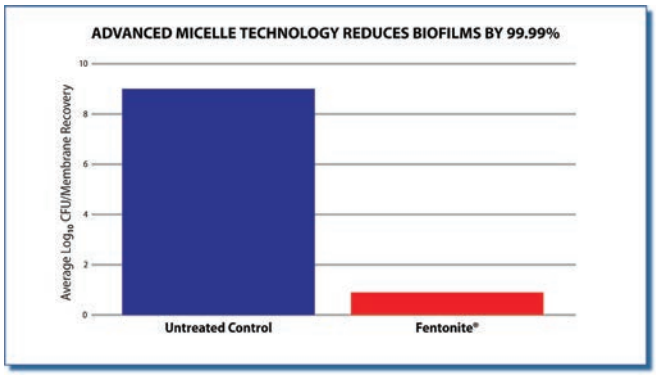

Figure 12

extracted by vortexing/sonicating, and extracted biofilm samples will be plated onto agar. Three replicates of each test article will be evaluated with paired untreated control replicates. Mean log10 and mean percent reductions attributable to each test article will be calculated relative to paired untreated control replicates. (Figures 11 & 12)

Drip Flow Biofilm Reactor® Test Method

In this method, a laboratory biofilm is established in batch mode for six hours and is then grown under low shear in continuous flow conditions for 48 hours. Biofilm accumulation is quantified by harvesting the biofilm from coupons of a known surface area, disaggregating the cell clumps, and performing viable plate counts.

The DFR consists of a rectangular base (various materials available) held at a 10° angle by an anodized aluminum stand, Figure 1. Four or six separate channels are bored into the base, resulting in independent sampling opportunities for each run performed. Each channel has two small pegs to hold the 18.75 cm2 (25 x 75 x 1mm) glass coupon in place, a shallow trough that mitigates blockage of the effluent port during sloughing events and aids in coupon removal, and an effluent port that allows the continuous flow media to exit. Each channel also has an alternant influent port that can be used for catheter studies. The covers contain rubber O-rings to

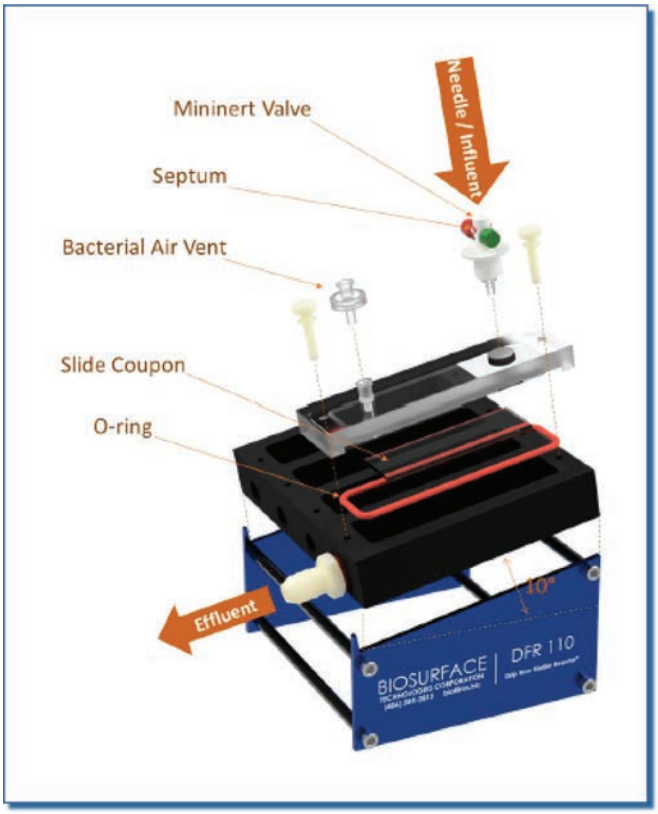

Figure 13

form an airtight seal, bacterial air vent gas exchange ports, and a Mininert Valve used for the inlet. The Mininert Valve consists of a rubber septum, into which a needle is placed to deliver the media, and

a ported bottom to allow more significant drops of media to form than possible with the needle alone. The flow of media is the only acting shear force on the biofilm.[28] (Figure 13)

Using Excessive Iron to Regulate Wound Bacteria

Bacteria sequester iron in their biofilms to protect themselves from the damage associated with excess "free" iron. When a bacterial cell gets too much iron, it has several consequences that negatively affect its physiology, metabolism, and viability. Iron is an essential nutrient for bacteria and necessary for various cellular processes such as DNA replication, respiration, and synthesizing critical cofactors like heme and iron-sulfur clusters. However, excess iron in bacterial cells harms physiology and viability by inducing oxidative stress through the Fenton Reaction, disrupting iron homeostasis, inhibiting growth, activating stress responses, and impairing autoinducers and virulence.

Excess iron, caused by the freeing of sequestered iron, disrupts these processes and induces oxidative stress. The potential outcomes of iron overload in bacterial cells include:

1. Oxidative Stress: Excess iron produces reactive oxygen species (ROS) through the Fenton Reaction. In this process, iron reacts with hydrogen peroxide to generate hydroxyl radicals. ROS are highly reactive and damage bacterial cellular components such as DNA, proteins, and lipids, leading to cellular dysfunction and cell death.
2. Disruption of Iron Homeostasis: Bacteria regulate iron uptake and storage to maintain iron homeostasis. Iron overload disrupts this balance, leading to the dysregulation of iron-dependent processes and cellular toxicity.
3. Inhibition of Growth: High iron levels inhibit bacterial growth by interfering with essential metabolic pathways. For example, excess iron inhibits the tricarboxylic acid (TCA) cycle enzymes, affecting cellular respiration and energy production.
4. Impaired Virulence: Iron is often a limiting nutrient for bacterial pathogens during infection. Bacteria have evolved sophisticated mechanisms to acquire iron from host tissues. However, excessive iron accumulation within bacterial cells impairs their ability to scavenge iron from the host environment, compromising their virulence and pathogenicity.

Bacteria obtain iron through the destruction of macrophages. Bacteria's iron requirements and ability to get this nutrient from the body's immune system form the genesis of bacterial infection. When bacteria have an abundance of iron, the need to scavenge for iron from macrophages is eliminated. The wound environment's immune system can react to the bacteria in full force, thus eliminating the risk of infection.[23]

Clinical Outcomes with Fentonite and BioBlock

The use of bioelectric nanoparticle wound dressings was studied over two years—a comprehensive selection of patients allowed for a broad-based evaluation of the products. The study required the development of a new standard of care document. Significantly, from an economic standpoint, the facility reduced the number of products in inventory by more than 90%. This alone represented a substantial savings. The reduction in treatments included amniotic tissue and antibiotics. The study was conducted by Michael Lavor, MD, medical director of Saguaro Wound Care Clinic in Tucson, Arizona. (Figure 14)

Patients	198
In Office Treatments	3,353
At Home Treatments	10,050
Length of Use (months)	23
Wound Type(s)	Traumatic and Post surgical
Wound Demographic	80% Chronic, 20% Acute
Healing Improvement	Wounds healed 40-60% faster with BioBlock™ Technology compared to our former standard of care
Pain Reduction	Decrease in pain in 95% of patients within first week
Notes	Less drainage within 2 weeks

Figure 14

One of the most exciting outcomes came from patient comments. An unexpected outcome was the reduction in pain. While research in this area is ongoing, scientific reasons still need to be discovered.

Advanced Products Require Economic and Social Consideration

Bringing new medical products to market requires years of research and development and substantial financial investments. Advanced products are subject to FDA review and approval. While the approval process is vital to ensuring products are safe and effective, it must address the economics of a new product's return on investment or affordability.

To be successful in today's medical product marketplace, a product must be affordable, improve healing outcomes, ensure easy patient compliance, and demonstrate improved healing times.
The fentonite and BioRelese products were tested over two years on 198 patients. The products substantially reduced healing times and medical costs. Below is a sampling of outcomes for five patients from the study.

Patient Economic Study 1

BL was an 81-year-old patient with a history of severe comorbidities. At the time of treatment, she suffered from Acute Chronic Systolic CHF, Acute PE, Multiple open Wounds in bilateral low extremities, Moderate protein-calorie malnutrition (HCC), Hypercholesterolemia, S/P MVR (mitral valve replacement), UTI (urinary tract infection), Sepsis (HCC), Pacemaker implanted.[29]

Previous costs and treatments 2016 - July 2022 (5 years) have included:

1. Amniotic Tissue on at least three different occasions, totaling over $200,000.
2. Dermal skin used on at least three occasions totaling at least $80,000.
3. Hyperbaric chamber, Infliximab, Warton's jelly injections, accurate relief treatments over $120,000.
4. Multiple operating room debridements cost over $200,000.

Approximate total: $800,000

New Treatment Protocol:

The patient was changed to
BioRelese
Fentonite (AgFresh)

The wounds were cleaned, and dressings were changed 3x a week.

Results After Three Months of Treatment/

1. Two wounds were entirely resolved.
2. Two wounds have been reduced by 60-70% in size, and healthy viable tissue can now be seen over the entire area of each wound.
3. The total product cost to date is around $1,300.
4. Weekly office visits are $7,500.
5. Treatment will continue to resolve the remaining wounds fully.

Approximate total: $8,800

The original product treatment was 3.33x more expensive than the McCord System per month, and the McCord System healed 26x faster!

8/28/22

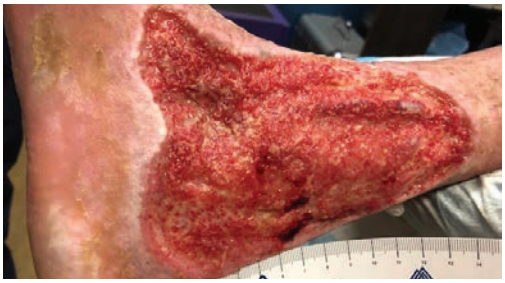

11/8/22

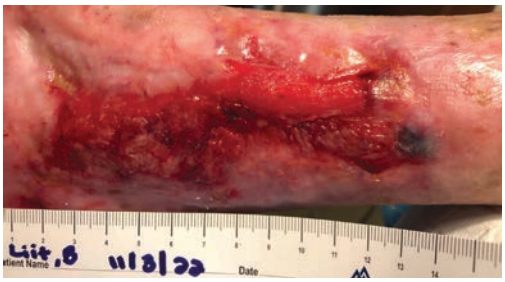

2/22/23

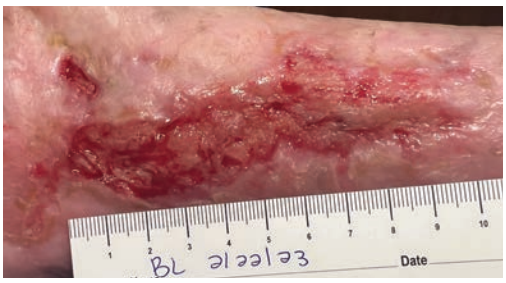

Patient Deceased – Study Concluded

Patient Economic Study 2

NS is a 76-year-old patient with comorbidities who had an ulcer recurring two times on the heel. The estimated healing time for the wound was six months before starting with a previous treatment plan.[30]

Previous costs and treatments lasted six months:

1. Office Visits: $2,976

2. Debridement Costs: $3,120

3. Product Cost: $500

Approximate total: $6,596

New Treatment Protocol:

The patient was changed to:

BioRelese
Fentonite (AgFresh)

The wounds were cleaned, and dressings were changed 3x a week.

Costs After Two Months of Treatment

1. Office Visits: $992

2. Debridement: $999

3. Product Cost: $300

Approximate total: $2,234

The original treatment was equal in price to the McCord system, but the McCord system healed 3x faster!

11/15/22

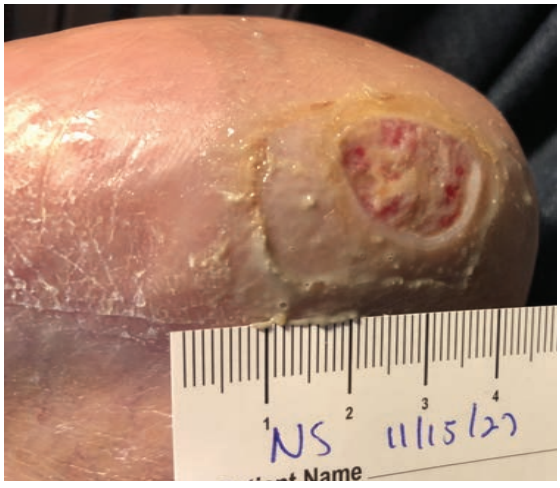

12/12/22

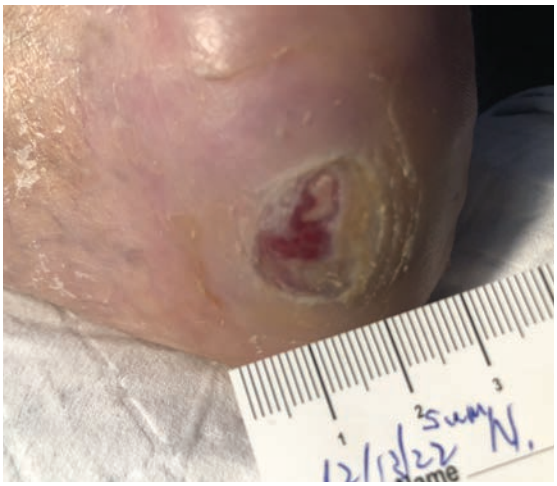

12/28/22

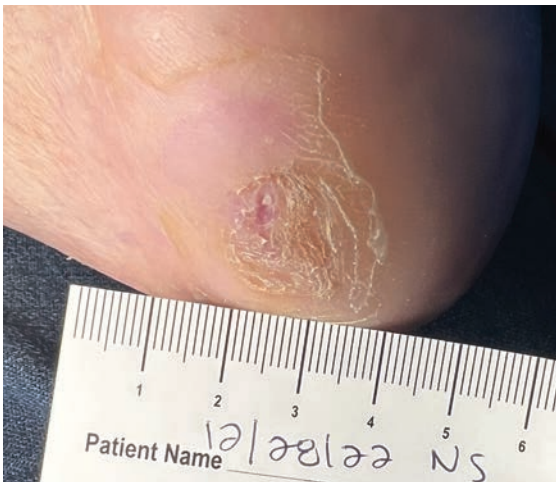

Patient Economic Study 3

EG has paraplegia with a stage 4 sacral ulcer that has been treated since 2017 with no significant improvement. The patient was treated with standard care and wound VAC before starting Fentonite and BioRelese.[31]

Previous costs and treatments lasted six years:

1. Office Visits: $57,600

2. Home Healthcare: $150,000

3. Debridement Costs: $60,200

4. Wound VAC: $9,000

5. Product Cost: $14,400

Approximate total: $291,200

New Treatment Protocol:

The patient was changed to:

BioRelese
Fentonite (AgFresh)

The wounds were cleaned, and dressings were changed 3x a week.

Costs After Six Months of Treatment

1. Office Visits: $2,480

2. Debridement: $4,560

3. Product Cost: $1,000

Approximate total: $7,040

The original treatment was 3.5 times more expensive per month than the McCord System, and the McCord System healed 12 times faster!

12/16/21

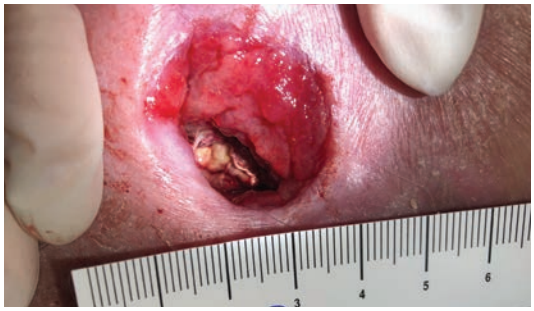

5/15/22

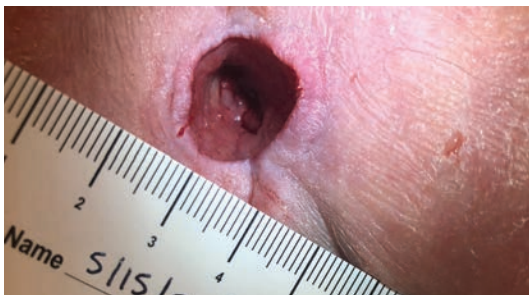

9/17/22

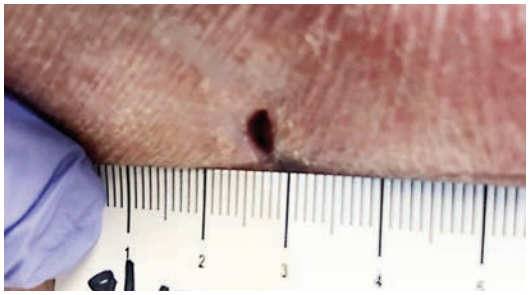

Patient Economic Study 4

AW had a surgical procedure for her back that became infected, and the hardware had to be removed. The patient's chronic wound was being treated for five years with the standard of care with no significant improvement.[32]

Previous costs and treatments lasted five years:

1. Office Visits: $24,800

2. Debridement Costs: $25,900

3. Product Cost: $14,400

4. Surgery Cost: $110,000

Approximate total: $175,100

New Treatment Protocol:

The patient was changed to:

BioRelese
Fentonite (AgFresh)

The wounds were cleaned, and dressings were changed 3x a week.

Costs After Four Months of Treatment

1. Office Visits: $1,984

2. Debridement: $2,400

3. Product Cost: $400

Approximate total: $4,684

The original treatment was 2.5 times more expensive per month than the McCord System, and the McCord System healed 15 times faster!

8/23/22

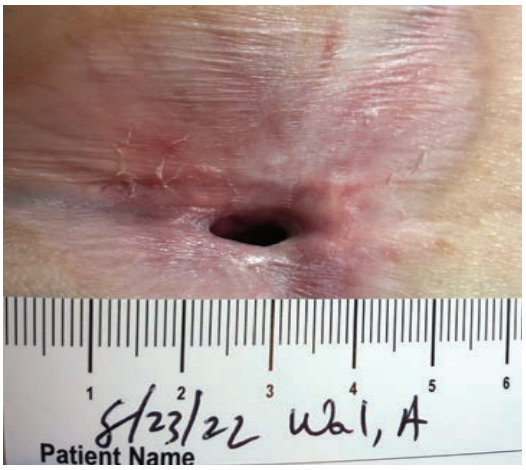

11/11/22

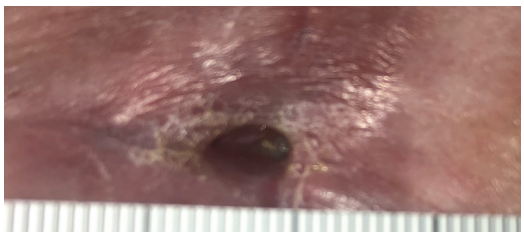

11/18/22

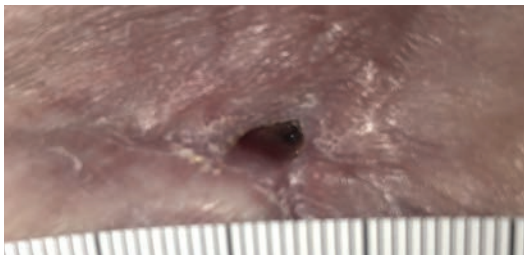

Patient Economic Study 5

MJP is an elderly female with a venous stasis ulcer that has been treated for ten years but has had no significant improvement. It was also excruciating, and she developed stricture of the Achilles tendon.[33]

Previous costs and treatments lasted ten years:

1. Office Visits: $57,040

2. Home Healthcare: $220,000

3. Debridement Costs: $77,000

4. Product Cost: $66,000

Approximate total: $420,040

New Treatment Protocol:

The patient was changed to:

BioRelese
Fentonite (AgFresh)

The wounds were cleaned, and dressings were changed 3x a week.

Costs After 12 Weeks of Treatment

1. Office Visits: $1,488

2. Home Healthcare: $6,000

3. Debridement: $1,500

4. Product Cost: $600

Approximate total: $9,588

The original treatment was 1.15x more expensive per month than the McCord System, and the McCord System healed 43x faster!

6/07/23

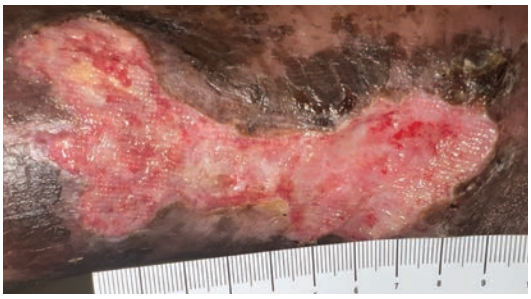

8/01/23

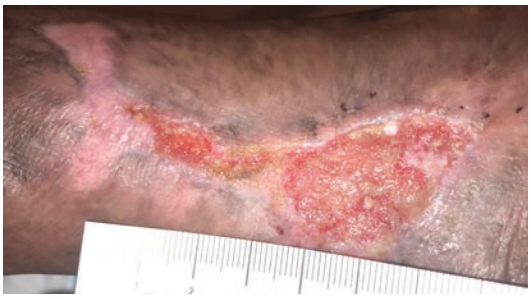

8/29/23

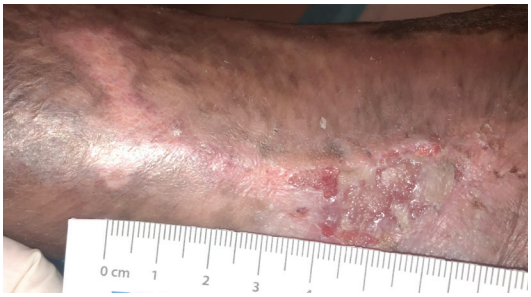

Conclusion

Cationic blends containing fentonite that form conductive bioelectric wound dressings hold immense potential for skin tissue engineering and wound repair. By integrating micelle-conductive scaffolds into tissue engineering, new bioelectric dressings that closely mimic the native electrical microenvironment of the skin have shown that stalled chronic wounds can be "energized" into renewed healing. These scaffolds provide structural support and serve as conduits for electrical cues, guiding cell behavior toward desired outcomes.

Fentonite bioelectric nanomaterial wound dressings offer opportunities for personalized medicine through their tunable electrical properties.

By adjusting parameters such as conductivity, electrical stimulation frequency, and waveform, we might tailor treatment modalities to suit individual patient needs, maximizing therapeutic outcomes while minimizing adverse effects.

Altered ionic charges, delivered topically to the wound bed without external stimulation, represent a paradigm shift in wound healing and skin tissue engineering. Ionic rebalancing provides the ability to harness the electrical cues necessary to promote tissue regeneration. Bioelectric nanomaterials have the potential to revolutionize the field of regenerative medicine, offering new hope for patients with chronic wounds and complex skin injuries.

References

1. Yu, R., Zhang, H., & Guo, B. (2021). Conductive biomaterials as bioactive wound dressing for wound healing and skin tissue engineering. Nano-micro Letters, 14(1). https://doi.org/10.1007/s40820-021-00751-y

2. Balint, R., Cassidy, N. J., & Cartmell, S. H. (2014). Conductive polymers: Towards a smart biomaterial for tissue engineering. Acta Biomaterialia, 10(6), 2341–2353. https://doi.org/10.1016/j.actbio.2014.02.015

3. Kiaee, G., Dimitrakakis, N., Sharifzadeh, S., Kim, H., Avery, R. K., Moghaddam, K. M., Haghiniaz, R., Yalcintas, E. P., De Barros, N. R., Karamikamkar, S., Libanori, A., Khademhosseini, A., & Khoshakhlagh, P. (2022). Laponite-Based nanomaterials for drug delivery. Advanced Healthcare Materials, 11(7). https://doi.org/10.1002/adhm.202102054

4. Naskar, A., & Kim, K. (2020). Recent advances in Nanomaterial-Based Wound-Healing therapeutics. Pharmaceutics (Basel), 12(6), 499. https://doi.org/10.3390/pharmaceutics12060499

5. Farber, P. L., Isoldi, F. C., & Ferreira, L. M. (2021). Electric factors in wound healing. Advances in Wound Care (New Rochelle, N.Y. Print), 10(8), 461–476. https://doi.org/10.1089/wound.2019.1114

6. Messerli, M. A., & Graham, D. M. (2011). Extracellular electrical fields direct wound healing and regeneration. The Biological Bulletin, 221(1), 79–92. https://doi.org/10.1086/bblv221n1p79

7. Zhao, M., Rolandi, M., & Isseroff, R. R. (2022). Bioelectric Signaling: Role of bioelectricity in directional cell migration in wound healing. Cold Spring Harbor Perspectives in Biology, 14(10), a041236. https://doi.org/10.1101/cshperspect.a041236

8. McCaig, C., Rajnicek, A. M., Song, B., & Zhao, M. (2005). Controlling cell behavior electrically: Current views and future potential. Physiological Reviews, 85(3), 943–978. https://doi.org/10.1152/physrev.00020.2004

9. Swerdlow, R. H. (2014). Bioenergetic medicine. British Journal of Pharmacology, 171(8), 1854–1869. https://doi.org/10.1111/bph.12394

10. Levin, M. (2012). Molecular bioelectricity in developmental biology: New tools and recent discoveries. BioEssays, 34(3), 205–217. https://doi.org/10.1002/bies.201100136

11. Wainwright, J., Hobbs, G., & Nakouti, I. (2021). Persister cells: formation, resuscitation and combative therapies. Archives of Microbiology, 203(10), 5899–5906. https://doi.org/10.1007/s00203-021-02585-z

12. Zegadło, K., Gieroń, M., Żarnowiec, P., Durlik-Popińska, K., Kręcisz, B., Kaca, W., & Czerwonka, G. (2023). Bacterial motility and its role in skin and wound infections. International Journal of Molecular Sciences (Online), 24(2), 1707. https://doi.org/10.3390/ijms24021707

13. Galdiero, E., De Alteriis, E., De Natale, A., D'Alterio, A., Siciliano, A., Guida, M., Lombardi, L., Falanga, A., & Galdiero, S. (2020). Eradication of Candida albicans persister cell biofilm by the membranotropic peptide gH625. Scientific Reports, 10(1). https://doi.org/10.1038/s41598-020-62746-w

14. Niepa, T. H. R. (2014). Electrochemical control of bacterial persister cells. Surface. https://surface.syr.edu/cgi/viewcontent.cgi?article=1077&context=etd

15. Mai, K., Maverakis, E., Li, J., & Zhao, M. (2023). Maintaining and restoring gradients of ions in the epidermis: The role of ion and water channels in acute cutaneous wound healing. Advances in Wound Care, 12(12), 696–709. https://doi.org/10.1089/wound.2022.0128

16. Keil, C., Hübner, C., Richter, C., Lier, S., Barthel, L., Meyer, V., Subrahmanyam, R., Gurikov, P., Смирнова, И., & Haase, H. (2020). CA-ZN-AG alginate aerogels for wound healing Applications: swelling behavior in simulated human body fluids and effect on macrophages. Polymers (Basel), 12(11), 2741. https://doi.org/10.3390/polym12112741

17. Meng, Y., Chen, L., Chen, Y., Shi, J., Zhang, Z., Wang, Y., Wu, F., Jiang, X., Yang, W., Zhang, L., Wang, C., Meng, X., Wu, Y., & Bu, W. (2022). Reactive metal boride nanoparticles trap lipopolysaccharide and peptidoglycan for bacteria-infected wound healing. Nature Communications, 13(1). https://doi.org/10.1038/s41467-022-35050-6

18. Patel, M., Kaneko, T., & Matsumura, K. (2017). Switchable release nano-reservoirs for co-delivery of drugs via a facile micelle–hydrogel composite. Journal of Materials Chemistry B, 5(19), 3488–3497. https://doi.org/10.1039/c7tb00701a

19. Alvarez-Lorenzo, C., & Concheiro, A. (2008). Intelligent drug delivery systems: polymeric micelles and hydrogels. Mini-reviews in Medicinal Chemistry, 8(11), 1065–1074. https://doi.org/10.2174/138955708785909952

20. Kotta, S., Aldawsari, H. M., Badr-Eldin, S. M., Nair, A. B., & Yt, K. (2022). Progress in polymeric micelles for drug delivery applications. Pharmaceutics (Basel), 14(8), 1636. https://doi.org/10.3390/pharmaceutics14081636

21. Bulutoglu, B., Acun, A., Deng, S., Mert, S., Lupon, E., Lellouch, A. G., Cetrulo, C. L., Uygun, B. E., & Yarmush, M. L. (2022). Combinatorial use of therapeutic ELP-Based micelle particles in tissue engineering. Advanced Healthcare Materials (Print), 11(13). https://doi.org/10.1002/adhm.202102795

22. Raghu, P. K., Bansal, K. K., Thakor, P., Bhavana, V., Madan, J., Rosenholm, J. M., & Mehra, N. K. (2020). Evolution of nanotechnology in delivering drugs to eyes, skin and wounds via topical route. Pharmaceuticals (Basel), 13(8), 167. https://doi.org/10.3390/ph13080167

23. Bird, L. J., Bonnefoy, V., & Newman, D. K. (2011). Bioenergetic challenges of microbial iron metabolisms. Trends in Microbiology, 19(7), 330–340. https://doi.org/10.1016/j.tim.2011.05.001

24. Hartman T. Cytotoxicity Evaluation of OBC-4 in Human Foreskin Fibroblasts. ImQuest BioSciences, Maryland. Project Number 642-02-02. 2021. https://mccordresearch.com/pages/case-studies

25. Aghajanian, A., & Aylozyan, K. ASTM E2315 - 16 Standard Guide for Assessment of Antimicrobial Activity Using a Time-Kill Procedure. Micro Quality Labs Inc., Accession #28532 Rev 1. 2021.

26. Ayala, M., & Zohrabyan, A. Antimicrobial Effectiveness Testing. Micro Quality Labs Inc., Sample: 6030. 2022.

27. Ayala, M., & Zohrabyan, A. Antimicrobial Effectiveness Testing. Micro Quality Labs Inc., Sample: 6015U. 2022.

28. Griggs, R. Evaluation of Three Test Articles for Their Ability to Prevent Formation of Biofilm Based on the Colony Drip Flow Biofilm Reactor Method. Final Report #2209498-903. 2022.

29. Frykberg, R., McCord, D., & Lavor, M. Anionic Chelation: A New Dynamic in Wound Care. https://mccordresearch.com/pages/case-studies

30. Frykberg, R., McCord, D., & Lavor, M. Improving Diabetic Foot Ulcer Closure Rates Using Fentonite AgFresh Hydrogel. https://mccordresearch.com/pages/case-studies

31. Frykberg, R., McCord, D., & Lavor, M. Treating a Quadriplegic's Non-Healing Wound with Fentonite-Based Products. https://mccordresearch.com/pages/case-studies

32. Frykberg, R., McCord, D., & Lavor, M. ThermoReversible Technology Provides a Pathway to Better Wound Outcomes. https://mccordresearch.com/pages/case-studies

33. Frykberg, R., McCord, D., & Lavor, M. After Suffering for 10-years With Unresolved, Painful Stasis Ulcer, MJP Was Healed in 12-Weeks and She Danced at Her Daughter's Wedding. https://mccordresearch.com/pages/case-studies

MR-0093